Deliverable No. 7.1 – Electrochemical characterization of LICs

AMAIA SÁENZ DE BURUAGA
BCARE

JON AJURIA
CICE

Deliverable No.	MUSIC D7.1	
Related WP	WP7	
Deliverable Title	Electrochemical Characterization of LICs	
Deliverable Date	2024-12-18	
Deliverable Type	REPORT	
Dissemination level	Public (PU)	
Written By	Amaia Sáenz de Buruaga (BCARE) Jon Ajuria (CICE)	2024-12-05
Checked by	Amaia Sáenz de Buruaga (BCARE)	2024-12-10
Reviewed by (if applicable)	María Arnaiz (CICE)	2024-12-16
Approved by	Jon Ajuria (CICE)	2024-12-18
Status	Final version	2024-12-18

Disclaimer / Acknowledgment

Publishable summary

WP7 will focus on the development of smart Sodium-Ion Capacitor (SIC) modules with integration of sensors and the Innovative – Supercapacitor Management System (i-SMS). The i-SMS concept is based on a management system that will include individual cell sensing of temperature, voltage and impedance, cell balancing, diagnosis algorithms and control and protection systems. The algorithms will include the estimation of State Of Charge (SOC), State Of Health (SOH) and State Of Power (SOP). The module will be developed according to the demands of the end-user and real-life conditions determined in the WP2 for railway application. Validation of the module will be conducted on a test bench simulating operational environmental and testing protocols defined in the WP2.

In order to speed up the work with SICs, as a first step, the above-mentioned development will be done for Lithium-ion Capacitors (LICs). A 12 V module will be developed using LIC cells, incorporating cell balancing, protections and diagnosis algorithms. With the aim of developing the corresponding i-SMS, it is important to know the behavior of the cells. Protections of the module will be established based on the operational safety limits of the cells. In addition, the electrochemical performance of the cells as well as the degradation profile needs to be analysed for the correct implementation of the algorithms.

For this purpose, the first task of this WP7 corresponds to the Task 7.1: Electrochemical characterization of Lithium-ion Capacitors. During this task, LIC cells from JTEKT manufacturer have been tested under different operating conditions to check their performance. For this purpose, the electrochemical performance of the cells under various temperatures and discharge currents has been tested, together with a thermal characterization. These tests will help to settle the safety performance limits to be used for the i-SMS protections. Additionally, floating tests have been conducted to study how the performance of the cells evolves under various operating conditions. The goal is to develop advanced algorithms that will enhance the efficiency and lifespan of the module.

This report presents a comprehensive overview of the results achieved from each test conducted. In terms of electrochemical performance, different temperatures and currents have been tested. According to the manufacturer, the cells are designed to operate in a wide range of temperatures and high currents. However, these technical characteristics need to be verified by laboratory tests. In this sense, for example, cells have shown poor performance when working at temperatures below 0 ºC. In addition, it is important to note that the high currents used by LICs can result in overheating, making effective thermal management crucial.

Finally, floating tests have also been carried out at three different temperatures. Having in-depth knowledge of how various electrochemical parameters evolve under different conditions over time enhances the accuracy of SOH, SOC, and SOP. However, even if 1400h of floating has been conducted at a high temperature (70 ºC), no cell degradation in terms of temperatures has been observed.

In conclusion, this report aims to summarize the different tests that have been carried out. Information derived from them will be used to develop the corresponding i-SMS for the 12V prototype LIC module including the corresponding estimation algorithms. However, due to the insufficient degradation observed, it will be necessary to analyze available databases and public information on similar technologies as alternative sources of insights.

Contents

List of Figures

List of Tables

List of Equations

Abbreviations

SYMBOL	SHORTNAME
BTMS	Battery Thermal Management System
EIS	Electrochemical Impedance Spectroscopy
ESR	Equivalent Series Resistance
LIC	Lithium-ion Capacitor
OCV	Open Circuit Voltage
SIC	Sodium-Ion Capacitor
SMS	Supercapacitor Management System
SOC	State Of Charge
SOH	State Of Health
SOP	State Of Power

1 Introduction

This deliverable is part of the WP7 "Innovative SMS, implementation and validation" and is part of the ask 7.1 "Electrical characterization of Lithium-ion capacitors". The aim of this deliverable, D7.1 "Electrochemical characterization of LICs" is to study the performance of Lithium-ion Capacitors (LIC) that later will be used to develop a 12V module.

1.1 Aim of the tests

The development of a robust and efficient LIC module requires an in-deep characterization phase at cell level. These tests allow for an extensive understanding of each cell's behavior under various operating conditions, which is crucial for designing a module that includes a Supercapacitor Management System (SMS), balancing mechanisms, protections, and advanced estimation algorithms.

First, characterization at different temperatures and currents provides detailed data on how the cells respond to extreme conditions and how their capacitance/capacity, internal resistance, and energy efficiency vary. These parameters are essential to ensure that the module can handle both high-charge conditions and prolonged discharges without compromising its performance or lifespan. Additionally, understanding LIC behavior within time allows to predict the module's long-term stability, which is critical in real applications to anticipate unplanned failures, simplify maintenance procedures as well as determine the problems responsible for malfunctioning or shortening the lifetime of the energy storage system.

The information obtained in these tests is essential for defining a protection system that enables safe operation of the module. Detailed characterization provides precise data on each cell's tolerances and limits, allowing the SMS and protection features to be configured to respond appropriately to over and under temperature, overcurrent and short-circuit, and over and under voltage. This way, the module can quickly react to any condition outside safe parameters, preventing unsafe conditions that could lead to cell failure.

Finally, these characterization tests aim to offer a solid foundation for developing advanced estimation algorithms, allowing the SMS to monitor the State Of Charge (SOC), State Of Health (SOH) and State Of Power (SOP) in real-time. The accuracy of these algorithms depends directly on the quality of the data obtained during characterization. A well-calibrated BMS with precise algorithms ensures reliable system monitoring, achieving more efficient energy management, extending the module's lifespan, and enhancing its performance in real-world operating conditions.

Thus, in this report, the different tests that have been carried out to the LIC cells will be summarized. First, a brief explanation of the cell's main technical parameters as well as the test descriptions will be given. Secondly, an in-deep explanation of the electrochemical and ageing tests performed and their results will be evaluated. Finally, the main conclusions of the data obtained will be given.

1.2 Cell technical information
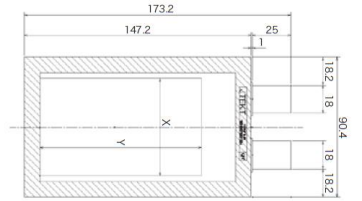
In order to carry out the electrochemical performance study, commercially available LIC cells from the Japanese JTEKT company were used. In Table 1 below, the main technical characteristics can be found:

Table 1. JTEKT cell main technical parameters

PARAMETER	VALUE	UNIT
Capacitance	1000	F
Capacity	0.444	Ah
Operating voltage range	2.2-3.8	V
Internal resistance	2.0	mΩ
Operating temperature range	-40 and 85 ºC (with operating voltage range from 2.2 to 3.8 V) *Note: After 1000 h float charging test (85 ºC, 3.8 V) internal resistance increase rate of 50% or less and capacitance reduction rate of 20% or less.*	ºC
	-40 and 100 ºC (with operating voltage range from 2.2 to 3.6 V) *Note: After 1000 h float charging test (100 ºC, 3.6 V) internal resistance increase rate of 50 % or less and capacitance reduction rate of 20 % or less.*	ºC
Cell weight	160	g
Cell volume	97	cm^3

In terms of the mechanical design of the cell, in the figure below it can be seen the geometry, tab positioning as well as the dimensions:

Table 2. JTEKT cell dimensions

		X: 63 mm Y: 111 mm t: 13.3 mm

1.3 Test description

1.3.1 Electrochemical tests

These electrochemical tests have been performed at different currents and environmental temperatures in the charge and discharge processes, while Open Circuit Voltage (OCV) and Electrochemical Impedance Spectroscopy (EIS) measurements are done periodically at different SOCs.

In the Table 3 below, the description of the different operating conditions tested can be checked:

Table 3. Description of electrochemical tests

Voltage window (V)	Temperature (ºC)	Currents (A)	Number of cycles	Tests
2.2-3.8	-40 ºC	6 A (<5 min) 20 A (<1.5 min) 40 A (40 s)	5 cycles at each condition	Measurement of EIS and OCV at 100%, 50 % and 0 % SOC
	-20 ºC			
	0 ºC			
	25 ºC			
	50 ºC			
	85 ºC			

As it can be checked, six different operating conditions have been tested, in order to check the performance of the cells at high and low temperatures, together with room temperature. In terms of the currents, the same current has been tested at charge and discharge. Three values have been tested, with time responses in the range of seconds or less than 5 minutes. For the EIS measurements the range of frequencies from 10 mHz to 10 kHz has been tested.

In terms of the ageing tests, floating tests have been carried out at different temperatures. In general, floating tests are based on continuous application of rated voltage at high temperature. Cells are usually kept at the upper category temperature limit and rated voltage for 1000 h or as agreed between both parts. As a reference for the definition of the tests, the standard IEC 62813:2015 – Lithium ion capacitors for use in electric and electronic equipment – Test methods for electrical characteristics has been considered.

Three different operating temperatures have been tested. In the Table 4 below the conditions have been summarized:

Table 4. Description of floating tests

Rated voltage (V)	Temperature (ºC)	Time (h)	Check-up	Number of cycles	Tests
3.8 V	70 ºC	1400 h	Every 100 h	10 Charge 12 A until 3.8 V and discharge at 12 A until 2.2 V	Measurement of EIS and OCV at 100%, 50 % and 0 % SOC
3.8 V	50 ºC	1400 h			
3.8 V	0 ºC	1400 h			

As it can be checked, three different temperatures have been tested, in order to check the degradation rate of the cells at different temperature conditions after approximately 1600

h at each temperature under floating conditions. In terms of the check-up, every 100 h, the 10 cycles have been carried out in order to check the capacitance evolution, as well as the evolution of EIS within time. For the degradation analysis, results will be given in terms on capacity due to processability for the algorithm development.

1.3.2 Thermal characterization

Additionally, it is important to consider that the high currents used by LICs can lead to overheating. As Soltani *et al.*[1] analysed, a thermal management system is crucial to maintain thermal stability and prolong the lifespan of the modules.

In this sense, in order to provide information on the thermal characteristics of the cells, some basic parameters at the cell level have been evaluated, such as the specific heat capacity (kJ kg^{-1} ºC^{-1}) or their thermal conductivity (W m^{-1} K^{-1}).

Specific heat capacity (C$_P$):

The objective of the methodology is obtaining the bulk specific heat (C_P) of the cell. Specific heat capacity is defined as the energy needed to increase a unit of mass of a substance by 1 K.

The methodology involves obtaining the cell C_P by comparing the thermal response of the actual electrochemical cell and an aluminium mockup of the same size when exposed to the same controlled temperature changes in a climatic chamber. The heat capacity of the aluminium mockup, which is well-characterized, is used as a reference.

In order to calculate the heat absorbed by the samples, an arrangement consisting of grouping two sample units with aluminium tape was instrumented with four K-thermocouples (error 0.5 %) as showed in Figure 1. The temperature measurements between the samples and at the surface will be used to calculate the absorbed heat during the heating program. Subsequently, the samples were introduced in a climatic chamber and subjected to the same heating program step from 20 °C to 70 °C. Two heating programs were carried out for each sample in order to ensure the consistency of the results.
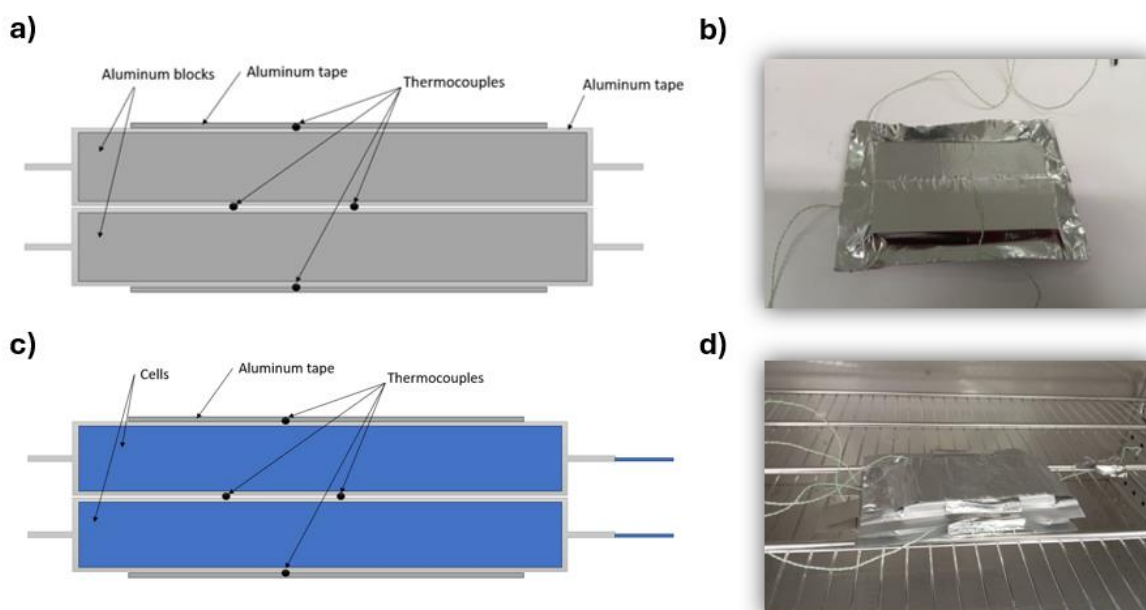

Figure 1. Testing samples arrangement: a) cross-section of the aluminium sample mockup, b) single instrumented aluminium block, c) cross-section of the two cells arrangement, and d) instrumented cells arrange

It is assumed that during the heating program both samples absorb the same amount of heat within the same time interval. This is a reasonable assumption because:

- The temperature evolution in the climatic chamber is the same.

- The surface temperature evolution of the two samples is very similar.

- The convection conditions inside the chamber are similar.

- The geometry, volume, and surface area of the cells and aluminium mockup are similar.

In those conditions the absorbed heat of the aluminium mockup ($Q_{Al\,mockup}$) will be as follows:

$$Q_{Al\,mockup} = m_{Al\,mockup} \cdot c_{P\,Al} \cdot \Delta T_{Al\,mockup}$$	**Equation 1**

Where $m_{Al\,mockup}$ is the total aluminium mass of the two aluminium blocks and tape, $c_{P\,Al}$ is the specific heat of aluminum 6082 T6 used and $\Delta T_{Al\,mockup}$ is the average temperature increase of the sample in the time step considered.

In the case of the cell arrangement, the heat absorbed (Q_{cell}) corresponds to the following expression:

$$Q_{cell} = m_{cell} \cdot c_{P\,cell} \cdot \Delta T_{cell} + m_{Al\,tape} \cdot c_{P\,Al} \cdot \Delta T_{Al\,tape}$$	**Equation 2**

Where m_{cell} is the total mass of the two cells, $c_{P\,cell}$ is the bulk specific heat of the cell, ΔT_{cell} is the average temperature increase of the cells, $m_{Al\,tape}$ is the mass of the aluminum tape used to attach the two cells, $c_{P\,Al}$ is the aluminum specific heat and $\Delta T_{Al\,tape}$ is the temperature increase of the aluminium tape.

Subsequently, considering that both arrangements absorb the same amount of heat, the following expression will be met:

$$\frac{Q_{cell}}{Q_{Al\,mockup}} = \frac{m_{cell} \cdot c_{P\,cell} \cdot \Delta T_{cell} + m_{Al\,tape} \cdot c_{P\,Al} \cdot \Delta T_{Al\,tape}}{m_{Al\,mockup} \cdot c_{P\,Al} \cdot \Delta T_{Al\,mockup}}$$	**Equation 3**

Where the $c_{P\,cell}$ can be obtained by isolating it from the equation as shown below:

$$c_{P\,cell} = \frac{m_{Al\,mockup} \cdot c_{P\,Al} \cdot \Delta T_{Al\,mockup} - m_{Al\,tape} \cdot c_{P\,Al} \cdot \Delta T_{Al\,tape}}{m_{cell} \cdot \Delta T_{cell}}$$	**Equation 4**

Thermal conductivity:

In the case of pouch format cells, the thermal conductivity is different along the in-plane and through-plane. In-plane conductivity refers to the thermal conductivity measured parallel to the material layers of the pouch cell. This direction aligns with the layers of electrodes, separators, and other components inside the cell. Through-plane conductivity refers to the thermal conductivity measured perpendicular to the material layers. This direction crosses through the stack of layers, from one face of the pouch to the opposite face.

Given the layered structure of the cells, heat can flow relatively freely in the in-plane direction (parallel to the layers) because it primarily travels along continuous, conductive materials like the current collectors (*e.g.*, aluminium and copper). In contrast, the through-plane direction (perpendicular to the layers), heat must cross interfaces that include separators and electrolytes with much lower thermal conductivity, thereby increasing thermal resistance.

To capture such an anisotropic thermal conductivity effectively, the Transient Plane Source (TPS)[1] technique is used. This method is based on the use of a flat disk-shaped sensor encompassing a double metal spiral. During the experiment, the sensor is placed between two pieces of the sample to be characterized and provides both thermal excitation (step heating) and temperature measurement. Parameters of the experiments and sensor size were chosen carefully following the guidelines from the standard Hot Disk ISO 22007-2:2015[2]. A Hot Disk TPS 2500S instrument was thus equipped with a Kapton sensor of 6.403 mm in radius (sensor type 5501 F1) positioned between two identical cells ensuring a flat and smooth contact surface and minimal air gaps, as shown in Figure 2.
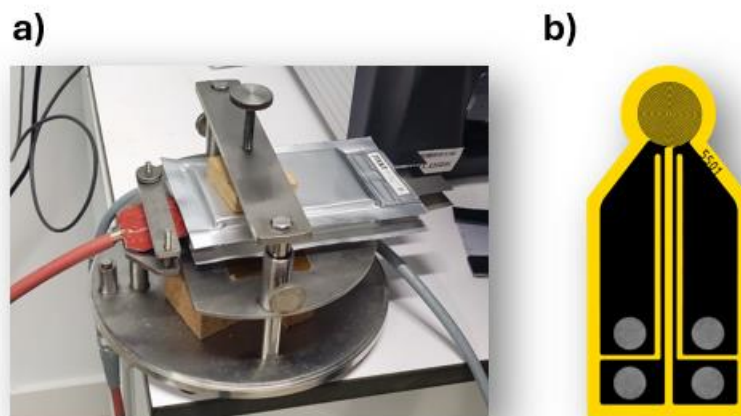
Figure 2. Testing sample arrangement: a) Experimental setup with the sensor placed between two cells, b) picture of 5501 F1 Kapton sensor.

Measurements were performed at room temperature (19 °C). The power applied to the sensor was set to 300 mW during 3 s. The temperature increase of the sensor can be determined by solving the heat conduction equation for an anisotropic semi-infinite medium[3]. In this configuration, the transient thermal behaviour of the cell can be modelled as follows[4]:

$$\Delta T(\tau_x) = P \left[\pi^{\frac{3}{2}} r \, (k_x k_z)^{\frac{1}{2}} \right]^{-1} D(\tau_x)$$

Equation 5

Where P is the power applied to the sensor, r is the radius of the latter, k_x and k_z are the thermal conductivities along the in-plane (x-axis) and through-plane (z-axis), respectively. Finally, $D(\tau_x)$ is a dimensionless time function which depends on the number of concentric rings of the sensor[5].

2 Methods and Results

2.1 Electrical characterization of Lithium-ion Capacitors (LIC)

2.1.1 Electrochemical characterization

Based on the operating temperature range declared in the cell datasheet, six different temperatures have been tested in order to check the discharged capacity in different operating temperatures. Moreover, three different discharged currents have also been tested, based on the time response expected of the system.

In the Figure 3 below, the discharged capacity for the different conditions can be analysed:
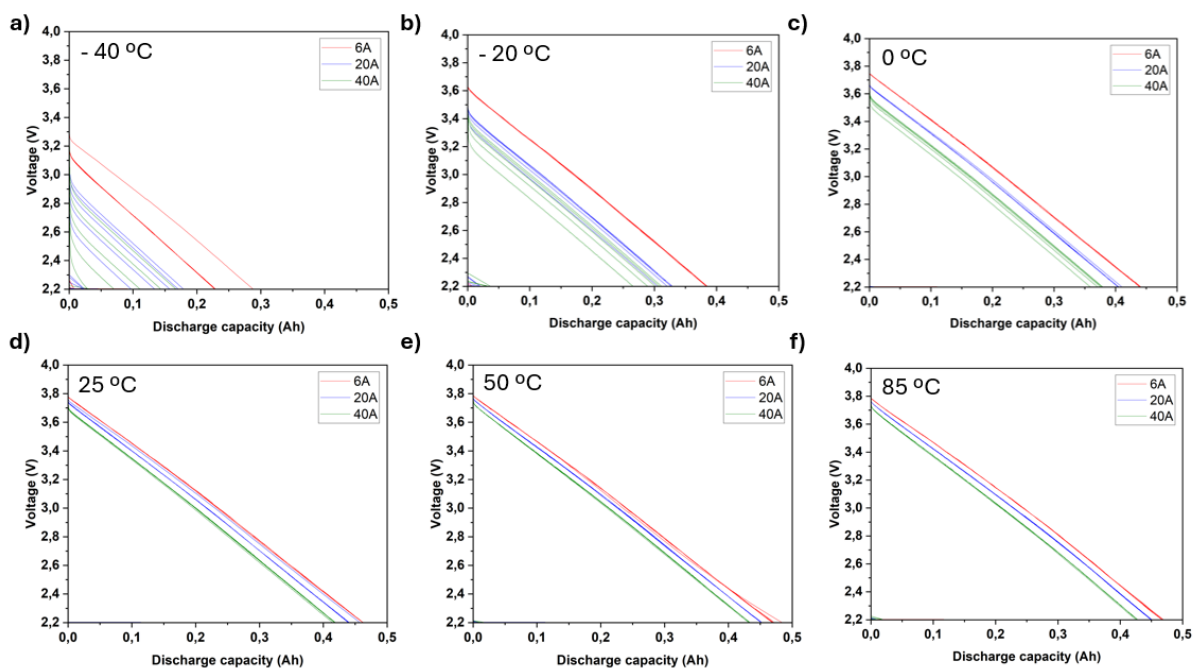
Figure 3. Discharge capacities at different currents and different operation temperatures a) - 40 ºC; b) - 20 ºC; c) 0 ºC; d) 25 ºC; e) 50 ºC; f) 85 ºC

As it can be seen, the discharged capacity decreases when higher current is applied. In addition, it can also be checked that among the 5 cycles, no differences in terms of discharged capacity are found when cycling at temperatures above 0 ºC. However, when cycling at lower temperatures, the discharged capacity is not homogeneous in all the cycles, thus, it can be concluded that the cell is not stable at low temperatures. In general, it can also be checked that the discharged capacity is much lower than the nominal capacity (0.444 Ah) when cycling at negative temperatures. At -20 ºC performance is still remarkable, however, at -40ºC the capacity fade is notorious, specially at high rates.

In the following Figure 4, the discharged capacity at different temperatures and currents can be checked. Two cells per condition have been tested in order to check the reproducibility of the obtained results:
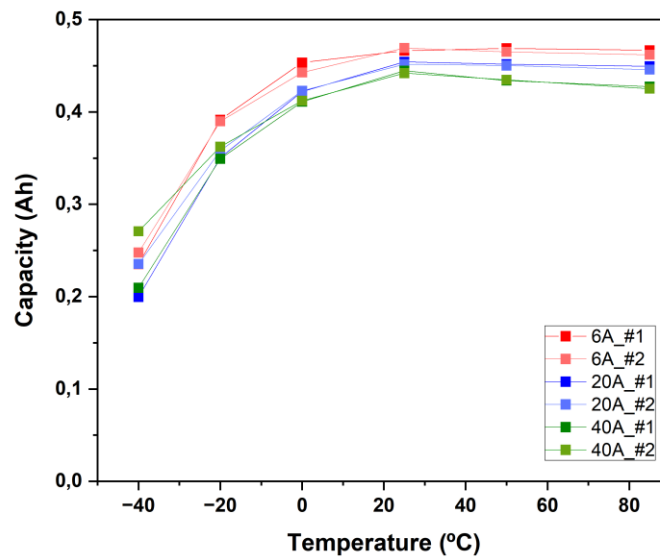
Figure 4. Discharged capacity at different temperatures and currents

As it can be seen, in general, good reproducibility has been found in the results. Moreover, when cycling at temperatures above 25 ºC, the discharged capacity corresponds approximately to the nominal capacity. However, when working at low temperatures, the capacity is decreased, reaching around half of the capacity when working at – 40 ºC. In addition, it should be pointed put that the results obtained at that temperature are not reproducible, which can indicate poor performance at temperatures below – 20 ºC. On the other hand, related to the applied currents, discharged capacity decreases as the applied current increases.

In addition to the capacity tests, Electrochemical Impedance Spectroscopy (EIS) tests have also been carried out:
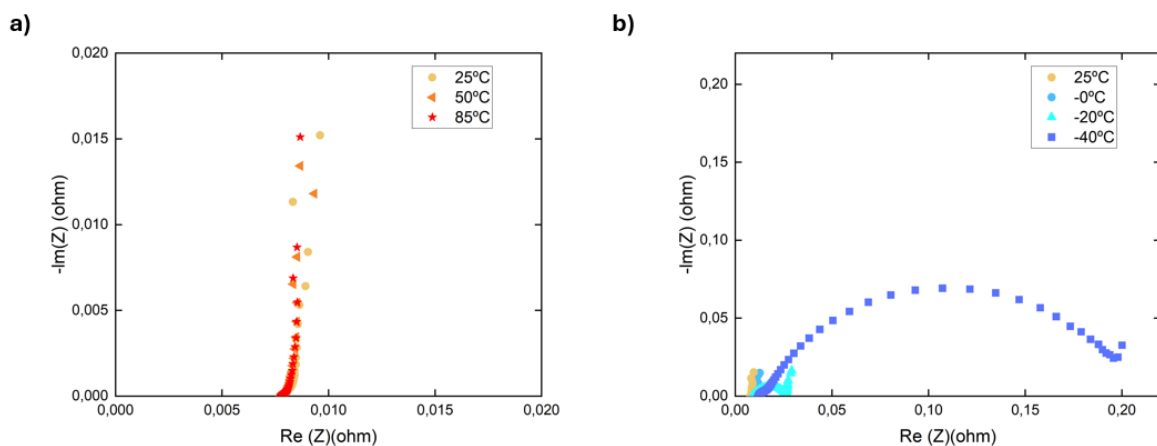
Figure 5. EIS spectra at different temperatures

In terms of the EIS spectra, it can be found in the Figure above that the curves obtained do not vary much within temperature when working at positive temperatures. However, when negative temperatures are applied (curves in blue), it can be checked how the charge transfer resistance increases significantly. This comes in agreement with the lower capacity obtained at low temperatures which can be found in Figure 3 and Figure 4.

Analysing the EIS spectra, the internal resistance value at different temperatures can be checked in the following Figure 6:
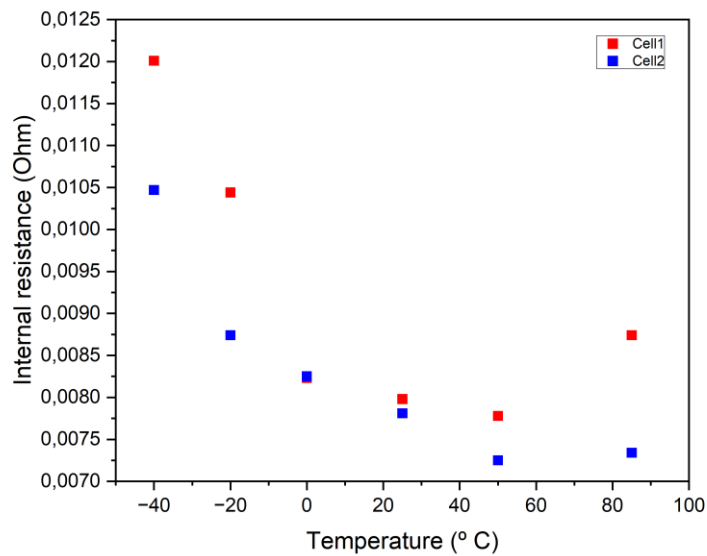
Figure 6. Internal resistance at different temperatures

The internal resistance is defined as the intersection of the Nyquist curve with the real resistance value (X axis) at high frequencies. In general, reproducible results can be found when working at temperatures between 0 ºC and 50 ºC.

In addition, EIS measurements were done at different SOCs in order to check differences in the results obtained. Three different values have been tested: 0, 50 and 100 % SOC. The Figure 7 below shows the internal resistance value at different temperatures and different SOCs.
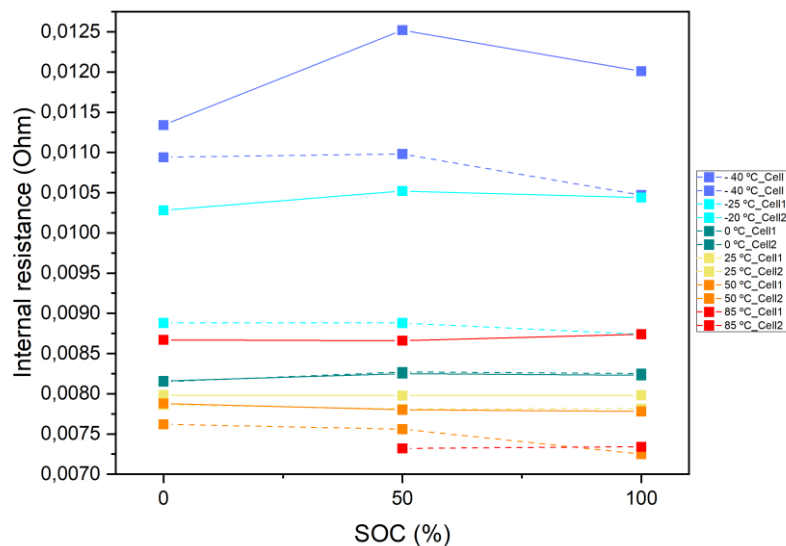
Figure 7. Internal resistance values at different SOCs and temperatures

Based on the data above, no differences can be found in terms of the internal resistance at different SOCs.

2.1.2 Thermal characterization

2.1.2.1 Heat capacity

The measurements carried out during the heating programs are shown in Figure 8. Due to the high thermal conductivity of aluminium, the temperature at the surface was very similar to the one at the inside of the two aluminium blocks, therefore only one temperature is plotted. Nevertheless, in the case of the cell arrangement, a non-negligible thermal gradient was observed. In addition, the average temperature increases in the cells that followed a slower rate, meaning that they have to present a higher specific heat. The temperature evolution within the climatic chamber follows a similar trend in both experiments. Besides, the surface temperature of both samples differentiates in no more than 3 °C. Therefore, a similar convection coefficient is expected and the assumption of both samples absorbing a very similar amount of heat may be correct.

Consequently, applying the equations showed above, the returned $c_{P, cell}$ is 1.40 J/g·K, with an error of ±0.07. $c_{P,Al}$ was assumed to be 0.891 J/g·K according to the material database MatWeb.com. The specific heat of an electrochemical cell depends on several intrinsic and extrinsic factors, namely, the material composition, cell structure, manufacturing variations, state of charge, or even the measurement methodology. This fact may lead to significant variations which highlight the need of carrying out a specific measurement for each study. In the present study, the value of 1.4 J/g·K is in the range of previously reported values of similar cells[6], with differences that may be attributable to any of the characteristics mentioned earlier.
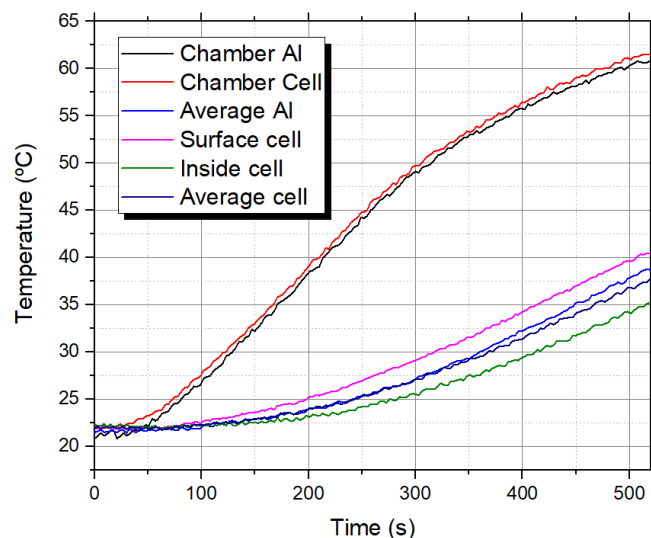
Figure 8. Experimental temperature measurements of the heating programs both for the Al mockup and cell arrangement

2.1.2.2 Thermal conductivity

It should be noted that, given its sequential nature, this method is sensitive to error propagation and, considering the complexity of the structure of the cell, can only lead to effective thermal properties estimation.

Figure 9 shows temperature increase as a function of time, which is related to the thermal properties of the surrounding material. Three different measurements are recorded for ensuring the repeatability of the measurement (tests 2 to 4). Then, the setup is

disassembled and assembled again to record another measurement (tests 1) to check the reproducibility of the setup. It is observed that the temperature increase recorded for the different tests present very similar results.

This temperature increase during the transient period is linearly proportional to a function $D(\tau_x)$. Accordingly, the characteristic time is used as a fitting parameter to calculate thermal diffusivity a_x along the x-axis. Next, the previously determined volumetric heat capacity (ρC_p) is required to calculate $k_x = a_x \rho C_p$. Finally, k_z is obtained from determined k_x and the slope of the line described in the above equation. The different test results are given in Table 5. Model and inverse method were programmed with Matlab® and its non-linear optimization toolbox.

Table 5. Thermal diffusivity and thermal conductivity results for the different tests

Test	a_x (mm²/s)	k_x (W/(m·K))	k_z (W/(m·K))
Test 1	12.3126	63.7711	0.25129
Test 2	12.5211	64.8510	0.24900
Test 3	12.3228	63.8759	0.25261
Test 4	12.3988	64.2180	0.25036

The obtained values are 64.18 $\pm$ 0.42 W/(mK) for in-plane conductivity and 0.250 $\pm$ 0.001 W/(mK) for through-plane conductivity. The uncertainty reflects the standard deviation across the four measurements.
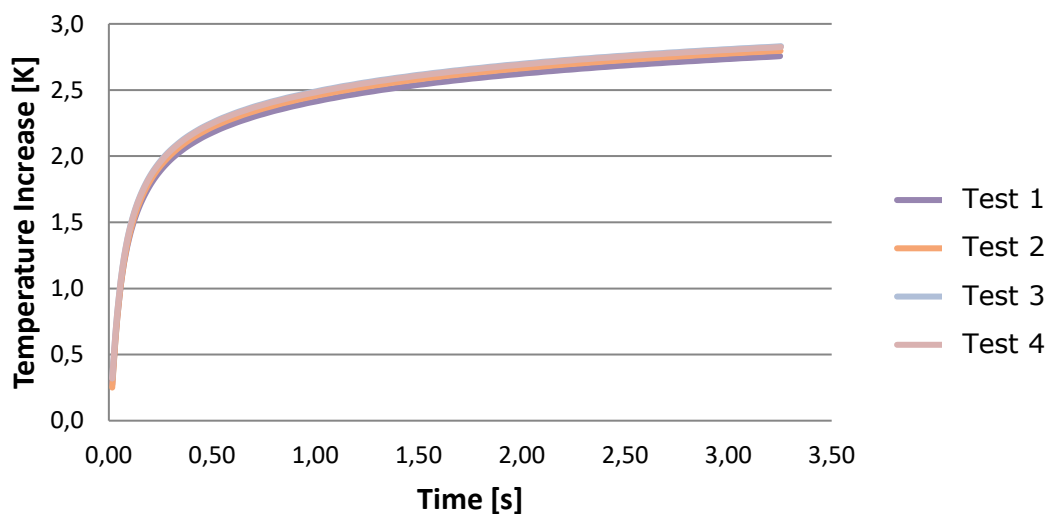

Figure 9. Transient temperature increase during the testing period

2.2 Ageing characterization

In order to check the degradation evolution of the cells at different operation conditions, long-term tests need to be carried out. Since by definition LIC cells have a cycle life of around 1M cycles[7], it was decided to subject the cells to floating tests at high and low temperatures.

2.2.1 Floating tests at 70 ºC

In a first step, it was decided to expose the cells to a high temperature ensuring the safety of the cells. Being 85 ºC the higher allowable operating temperature (or 100 ºC with reduced floating voltage of 3.6 V) declared by the manufacturer, and for safety concerns, it was decided to test under floating conditions at 70 ºC as the upper temperature limit.

2.2.1.1 Floating

Two cells have been tested at 70 ºC under floating conditions with periodical check-ups in order to get information about the degradation of the cells. For these tests, no pressure was applied to the cells. In the Figure 10 below, the floating results can be checked in which every 100h a check-up was done.
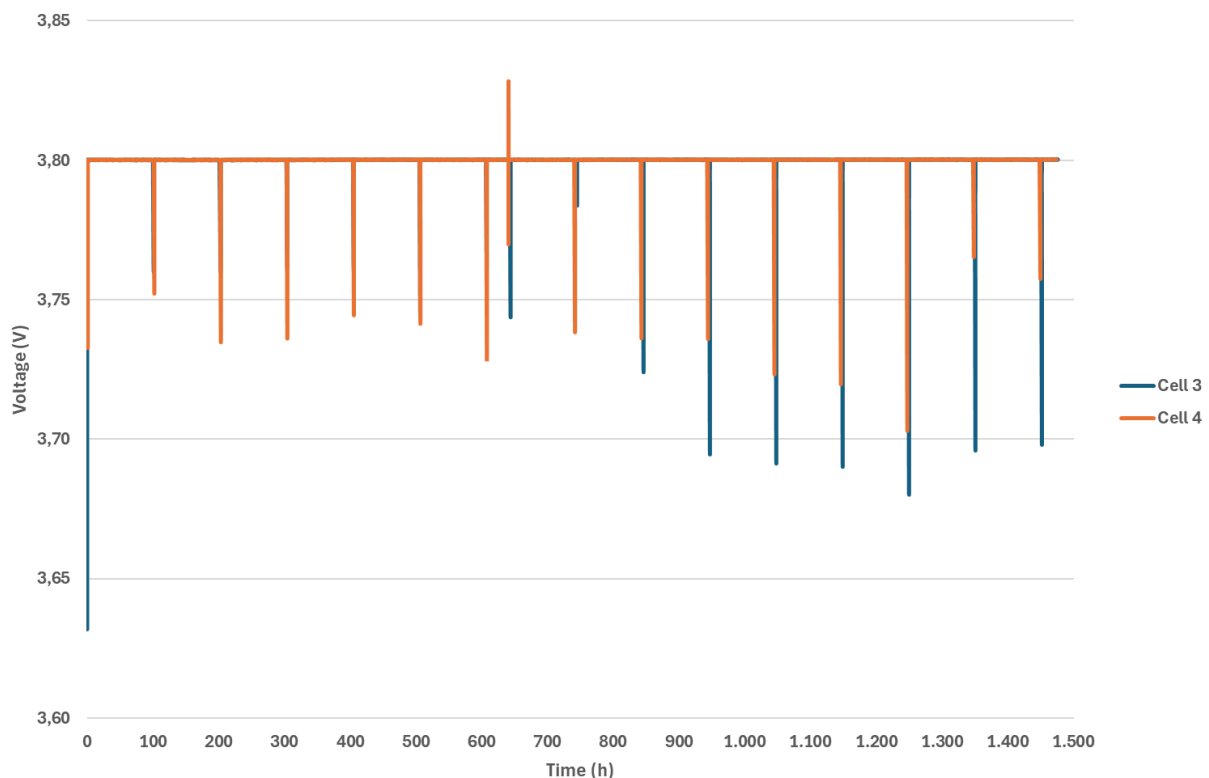
Figure 10. Floating test at 70 ºC for Cell 3 and Cell 4

In the figure above, it can be checked that cells were maintained at the upper voltage limit (3.8 V) for more than 1500 h. The voltage drop detected every 100 h corresponds to the periodical check-ups.

It should be noted that the voltage peak that can be observed at 600h is due to a break in cycling that had to be carried out for maintenance in the test laboratory. During this break, cells were maintained at 70 ºC and the connections were not modified in order not to change the impedance measurement.

2.2.1.2 Capacity evolution

During the periodical check-ups, first, 10 charge-discharge cycles were carried out at low currents (*i.e.,* 12 A). In the following Figure 11, where voltage vs time is represented, the last cycles of each check-up have been plotted.

a)

b)
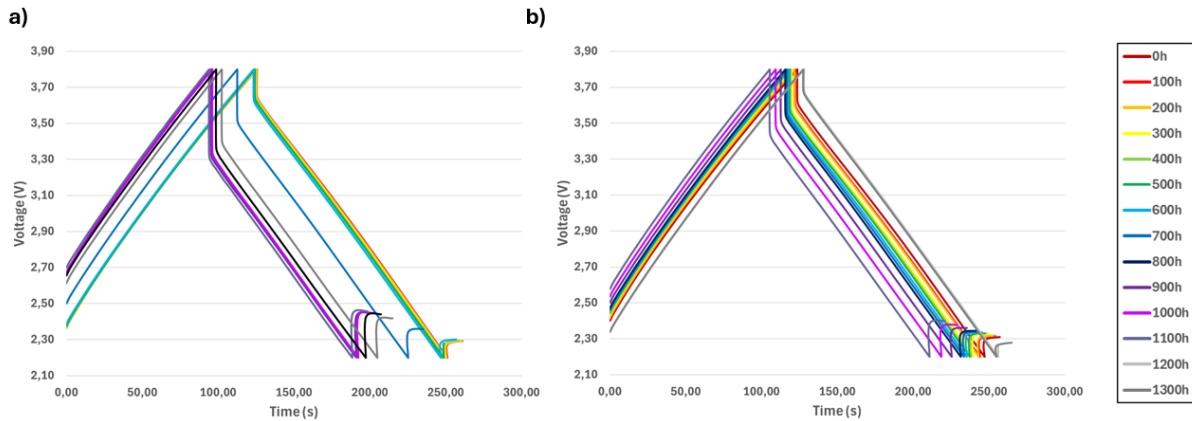
Figure 11. Charge-discharge profiles within time - a) Cell 3; b) Cell 4

As it can be checked in the Figure, there is a voltage drop increase over time due to an increase in the Equivalent Series Resistance (ESR).

2.2.1.3 EIS evolution

During the periodical check-ups, and after the 10 charge-discharge cycles, cells were discharged and EIS was measured in a wide range of frequencies at 0, 50 and 100 % SOCs with partial charges until the desired voltage values. In the Figure 12 below the different results can be found:
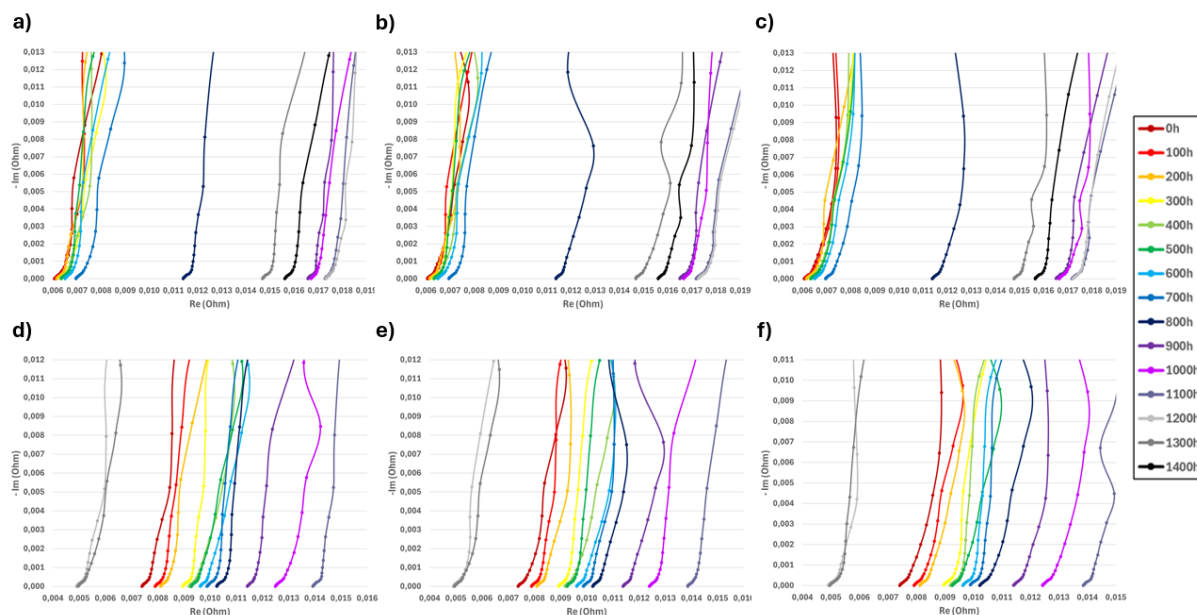
Figure 12. EIS spectra for Cell 3 at a) 0% SOC; b) 50% SOC and c) 100% SOC and Cell 4 at d) 0% SOC; e) 50% SOC and f) 100% SOC

In agreement with the Figure 11, in the Figure 12 it can be checked that internal resistance values increase over time. For these tests, no pressure was applied. However, in view of the results, and for the rest of the tests it was decided to apply pressure.

In terms of the differences of the curve within the time and SOC, the following figure shows the results obtained:
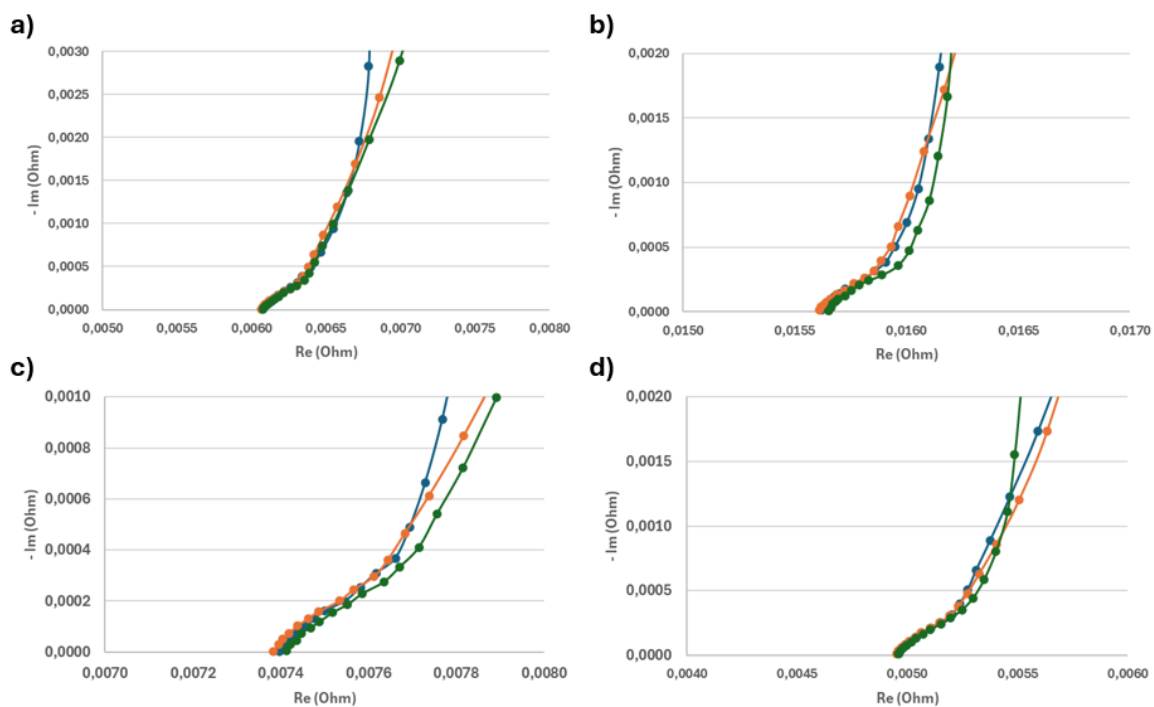
Figure 13. EIS curve evolution within time and SOC value - a) Cell 3 – Initial; b) Cell 3 - Final; c) Cell 4- Initial; d) Cell 4 - Final; Blue 0% SOC - Orange 50% SOC - Green 100% SOC

As it can be seen in Figure 13, at low frequencies, there is a curve shift that could be related to the SOC value and the interfacial impedance. However, further analysis in terms of frequencies, resistances values and reproducibility among the two cells needs to be done.

2.2.2 Floating tests at 50 ºC

Two cells were cycled under controlled temperature in a climatic chamber. For these tests, and as it has been said before, pressure has been applied to the cells in order to control the cell thickness changes.

2.2.2.1   Floating

Two cells have been tested at 50 ºC under floating conditions with periodical check-ups in order to get information about the degradation of the cells. In the figure below, the floating results can be checked in which every 100 h a check-up was done.
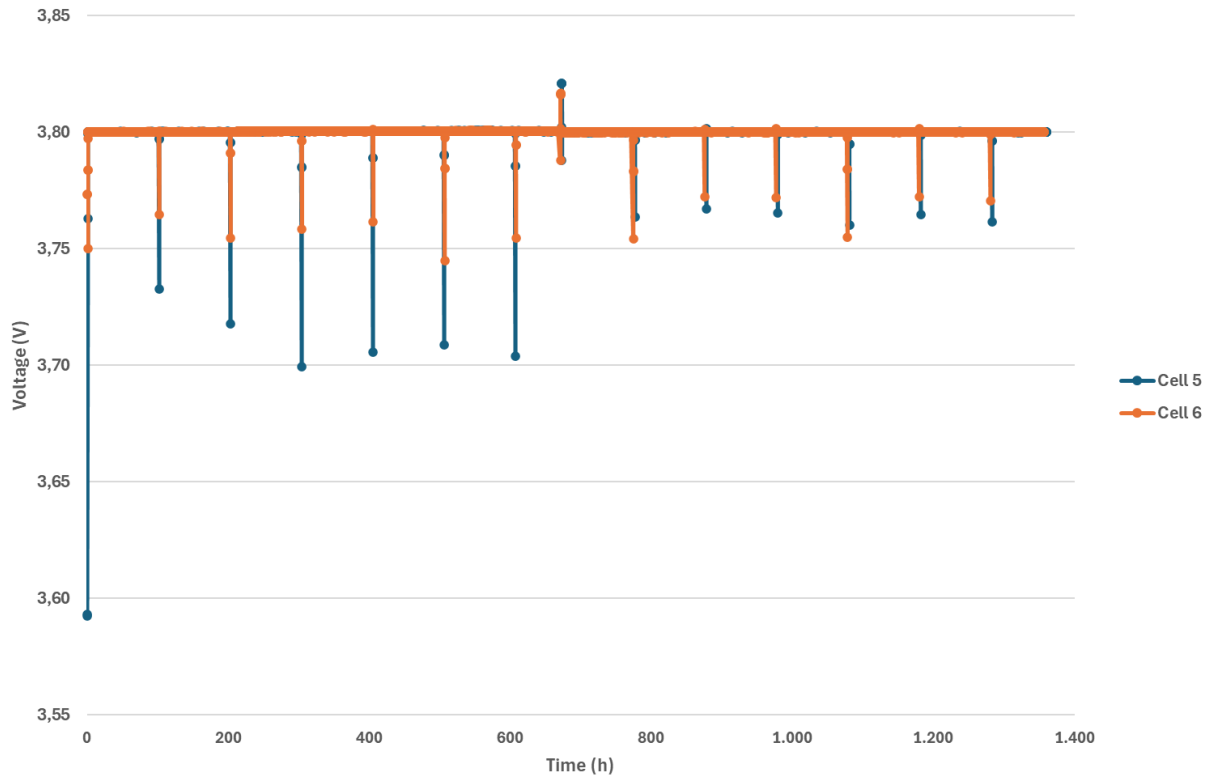
Figure 14. Floating test at 70 ºC for Cell 5 and Cell 6

In the Figure 14 above, it can be checked that cells were maintained at the upper voltage limit (3.8 V) approximately 1400 h. The voltage drop detected every 100 h corresponds to the periodical check-ups.

It should be noted that the voltage peak that can be observed at 700h is due to a chamber maintenance that was done during the tests in the testing laboratory. During this break, cells were maintained at 50 ºC and the connections were not modified in order not to change the impedance measurement.

2.2.2.2 Capacity evolution

During the periodical check-ups, first, 10 charge-discharge cycles were carried out at low currents (*i.e.,* 12 A). In the following figure, the last cycles of each check-up have been plotted.
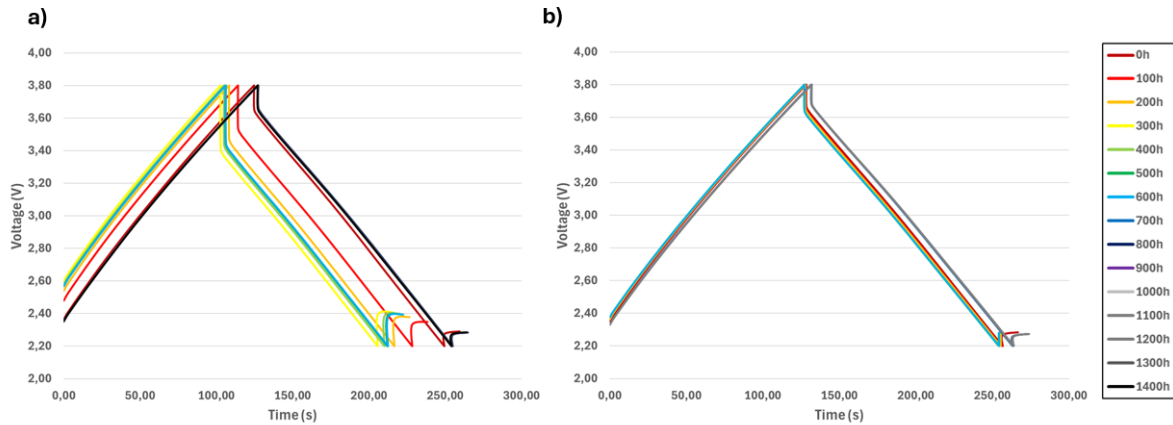
Figure 15. Charge-discharge profiles within time - a) Cell 5; b) Cell 6

As it can be checked in the Figure 15, there is a voltage drop increase over time due to an increase in the Equivalent Series Resistance (ESR). This increase in more appreciable in the first cell (Cell 5) which reflects the influence of the cell connection method in the internal resistance.

2.2.2.3 EIS evolution

As in the tests at 70 ºC, impedance measurements have been done at 0, 50 and 100% SOC from 10 mHz to 10 kHz, with partial charges until the desired voltage values. In Figure 16 below the different results can be found:
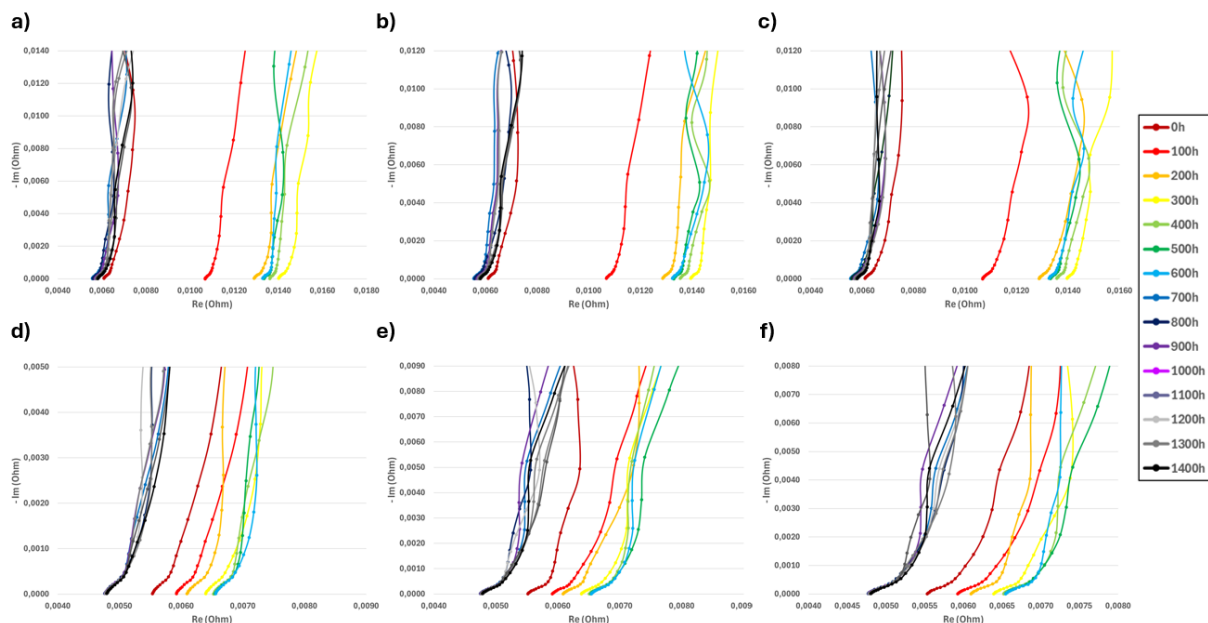
Figure 16. EIS spectra for Cell 5 at a) 0% SOC; b) 50% SOC and c) 100% SOC and Cell 6 at d) 0% SOC; e) 50% SOC and f) 100% SOC

In this case, it can be checked that during the first 600h, the internal resistance increased over time. However, after the climatic chamber maintenance was done, the internal resistance values decreased significantly. This might be related to connections, which were disassembled for the maintenance and mounting might have probably not been done on the exact way.

In terms of the differences of the curve within the time and SOC, the following Figure 17 shows the results obtained:

Figure 17. EIS curve evolution within time and SOC value - a) Cell 5 – Initial; b) Cell 5 - Final; c) Cell 6- Initial ; d) Cell 6 - Final ; Blue 0% SOC - Orange 50% SOC - Green 100% SOC

Similarly than in the case of 70 ºC tests, at low frequencies, there is a curve shift that could be related to the SOC value and the interfacial impedance. However, further analysis in terms of frequencies, resistance values and reproducibility among the two cells needs to be done.

2.2.3 Floating tests at 0 ºC

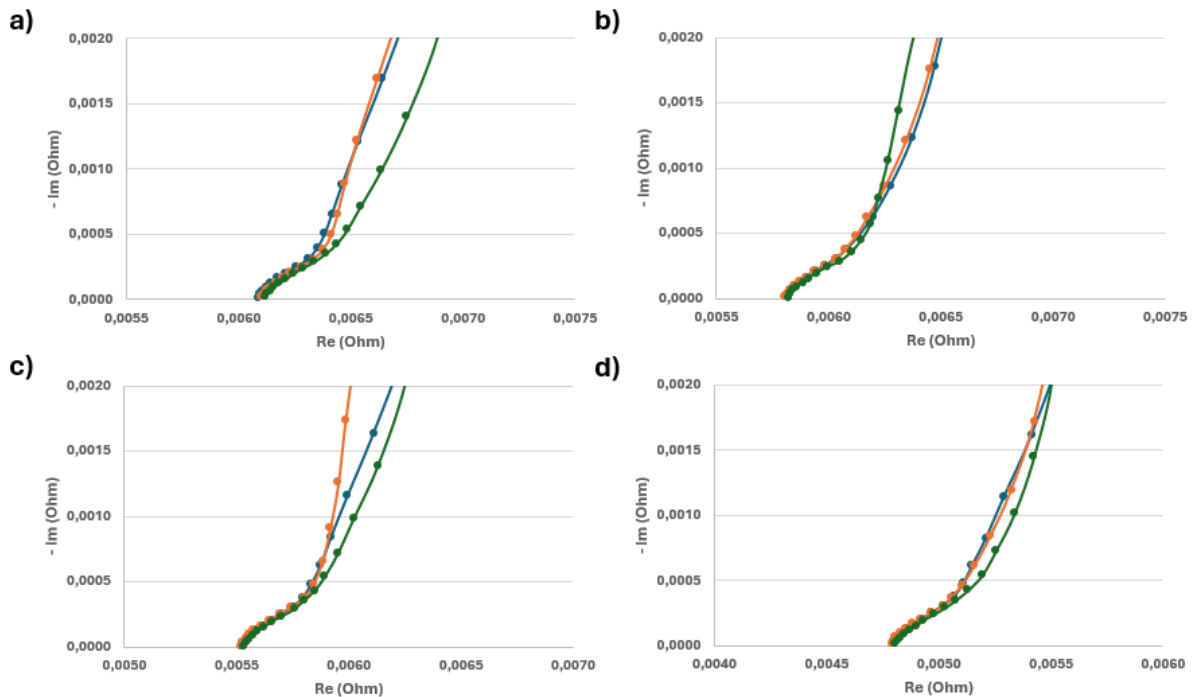During the electrochemical tests, it was determined that cells have a good performance when operating at temperatures above 0 ºC. However, when working at lower temperatures, the capacity obtained decreased significantly and the results were not reproducible between the two cells. Thus, in order to check the floating performance of the model at low temperatures, 0 ºC was defined since it is the lowest temperature at which reproducible results were obtained.

2.2.3.1   Floating

Two cells have been tested at 0 ºC under floating conditions with periodical check-ups in order to get information about the degradation of the cells. In the figure below, the floating results can be checked in which every 100 h a check-up was done.
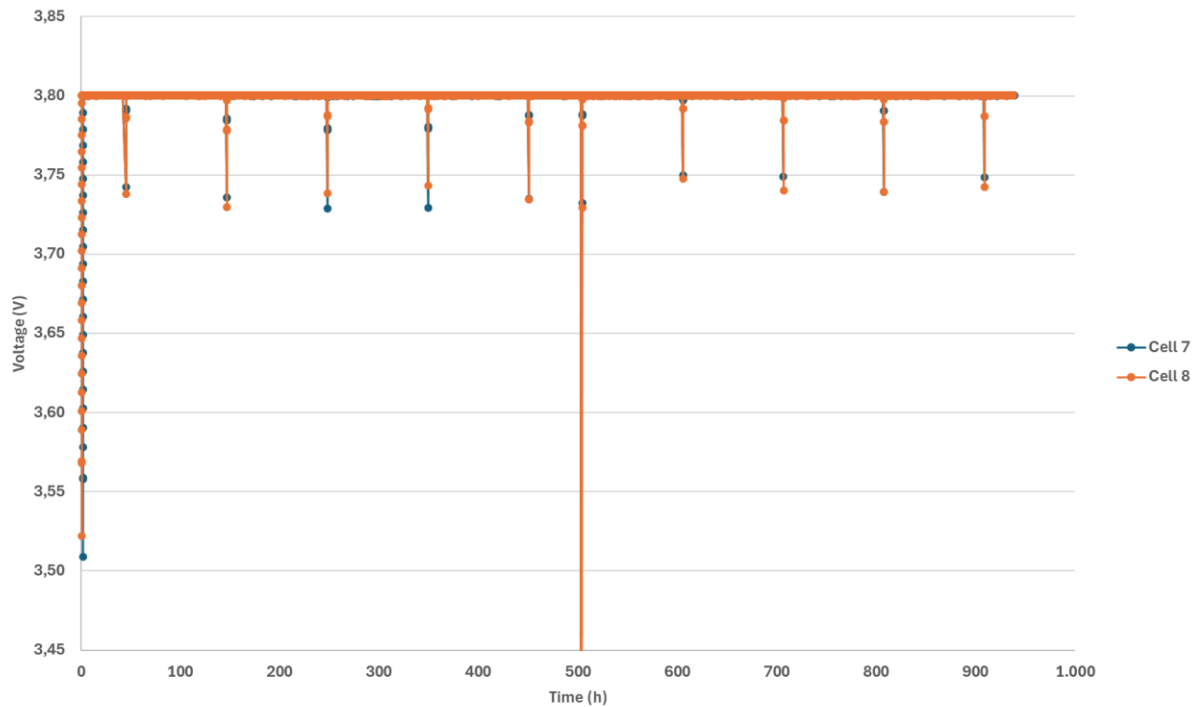
Figure 18. Floating test at 0 ºC for Cell 7 and Cell 8

In the Figure 18 above, it can be checked that cells were maintained at the upper voltage limit (3.8 V) approximately 1000 h. The voltage drop detected every 100 h corresponds to the periodical check-ups.

However, it should be noted that after approximately 600 h, the temperature of the chamber was changed to 25 ºC due to internal problems and thus, the cell performance varied. In terms of floating conditions, cells were maintained every time at the upper voltage limit.

2.2.3.2   Capacity evolution

During the periodical check-ups, first, 10 charge-discharge cycles were carried out at low currents (12 A). In the following Figure 19, the last cycles of each check-up have been plotted.

Figure 19. Charge-discharge profiles within time - a) Cell 7; b) Cell 8

In contrast of what is has been appreciable when testing at high temperatures, there is not much voltage drop increase at 0 ºC. In terms of charge and discharge profiles, not

appreciable changes can be found related to the temperature change produced at approximately 600 h of cycling.
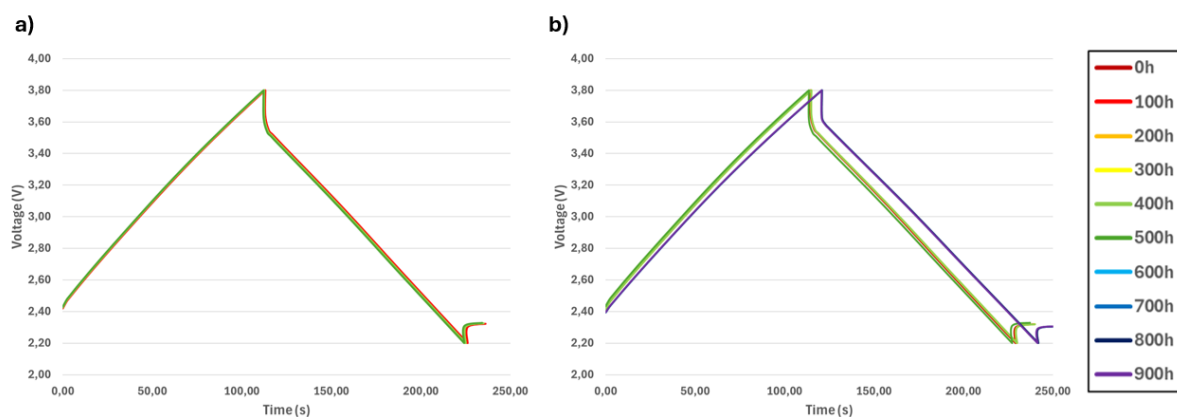
2.2.3.3 EIS evolution

As in the other tests, impedance measurements have been done at 0, 50 and 100 % SOC with partial charges until the desired voltage values. In the Figure 20 below the different results can be found:
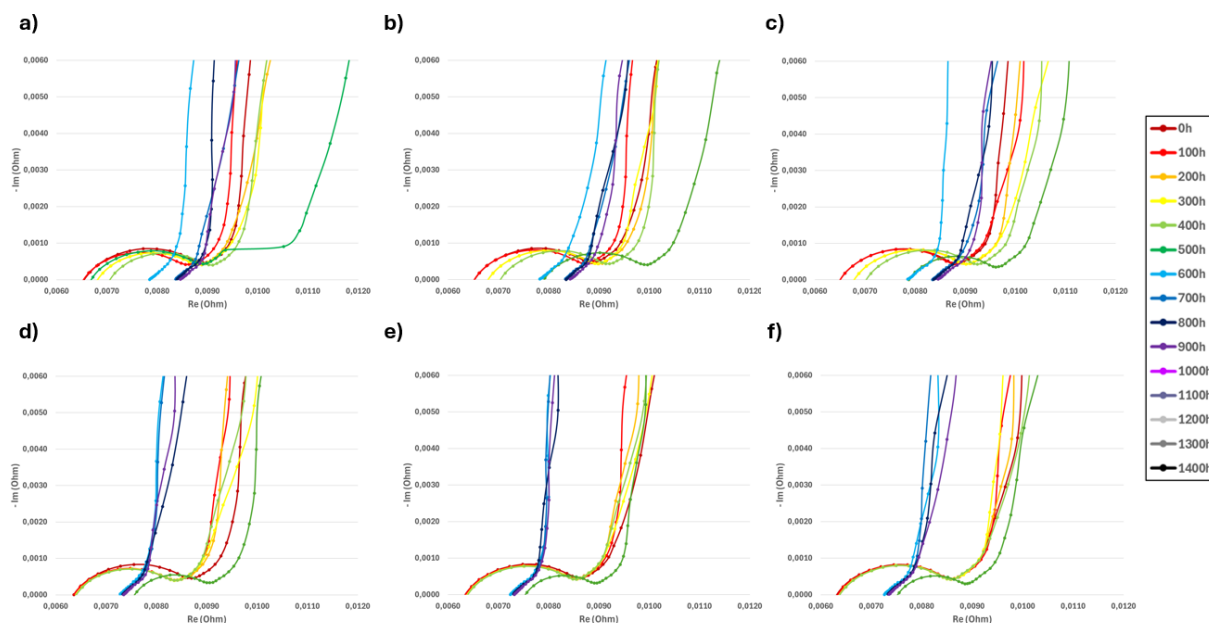
Figure 20. EIS spectra for Cell 7 at a) 0% SOC; b) 50% SOC and c) 100% SOC and Cell 8 at d) 0% SOC; e) 50% SOC and f) 100% SOC

In this case, it is very appreciable that the EIS curve shape changes at around 600 h, which is due to the climatic chamber change produced in which the temperature was changed from 0 ºC to 25 ºC. Thus, in the figure it can be seen that, at low temperatures, the charge transfer resistance is higher which could be attributed to a reduced mobility of the electrolyte ions. This enables to see the complete semicircle. However, from 600 h onwards, the EIS shape changes, with less semicircle.

In terms of the differences of the curve within the time and SOC, the following figure shows the results obtained. For this analysis the EIS curve at 500 h has been taken as the final curve since it is the last check-up before the climatic chamber change:
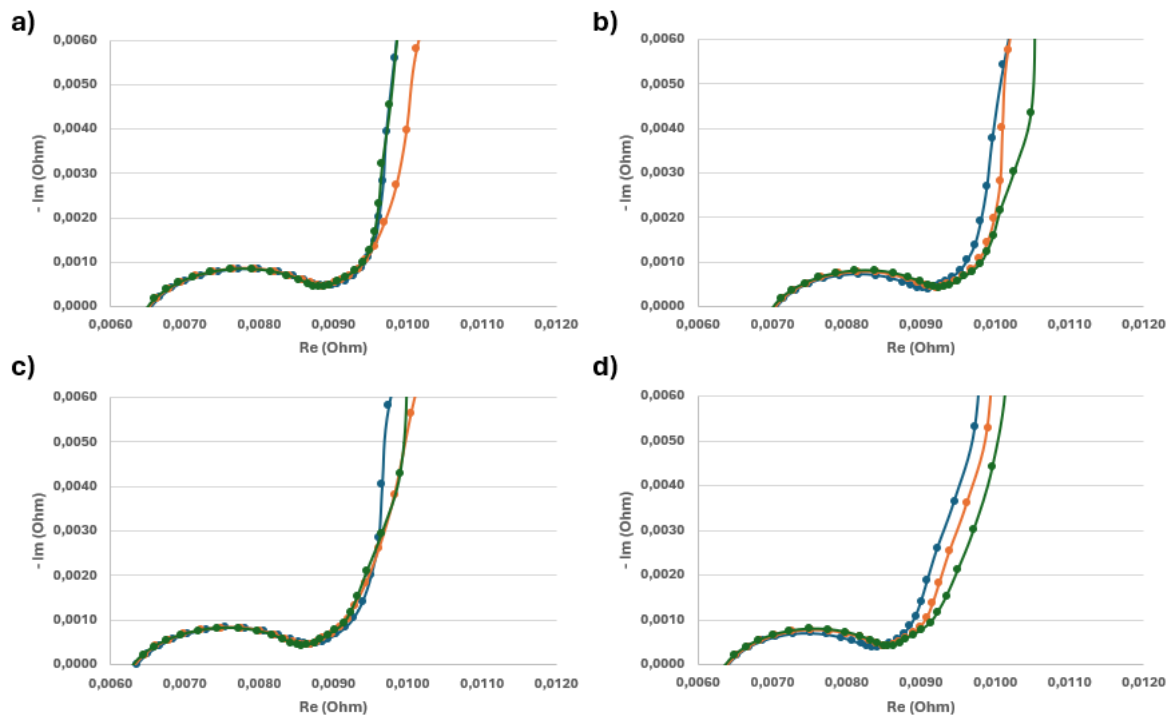
Figure 21. EIS curve evolution within time and SOC value - a) Cell 3 – Initial; b) Cell 3 - Final; c) Cell 4- Initial ; d) Cell 4 - Final ; Blue 0% SOC - Orange 50% SOC - Green 100% SOC

As it can be seen in the Figure 21, at this temperature, the complete Nyquist curve can be seen. Moreover, at low frequencies, it seems there is a curve shift that could be related to the SOC value and the interfacial impedance. However, further analysis in terms of frequencies, resistances values and reproducibility among the two cells needs to be done.

3 Discussion and Conclusions

During these tests, first of all, the cell performance under different operating conditions has been tested. In this sense, different temperatures as well as charge and discharge currents have been tested.

In terms of operating temperatures, according to the manufacturer's information, cells are supposed to work in a wide range of temperatures, from – 40 ºC to 100 ºC. However, it has been checked that cells have non-reproducible results when working at temperatures below 0 ºC as well as a lower discharged capacity. Nevertheless, concerning high operating conditions, cells have very good results even at 85 ºC with discharged capacities around the nominal capacity, thus, without capacity lose. No higher temperature has been tested due to safety concerns.

In terms of applied currents, a maximum of 40 A has been tested, even if the manufacturer claims a maximum discharge current of 200 A. However, due to safety concerns, 40 A was selected as the maximum current, which means time responses of 40 seconds. By analysing the results, it can be seen that the discharged capacity decreases when higher current is applied.

After the electrochemical characterization, floating tests were carried out at three different temperatures in order to analyse the degradation of the cells. The comparison of the obtained capacity degradation within time can be checked in the Figure 22:
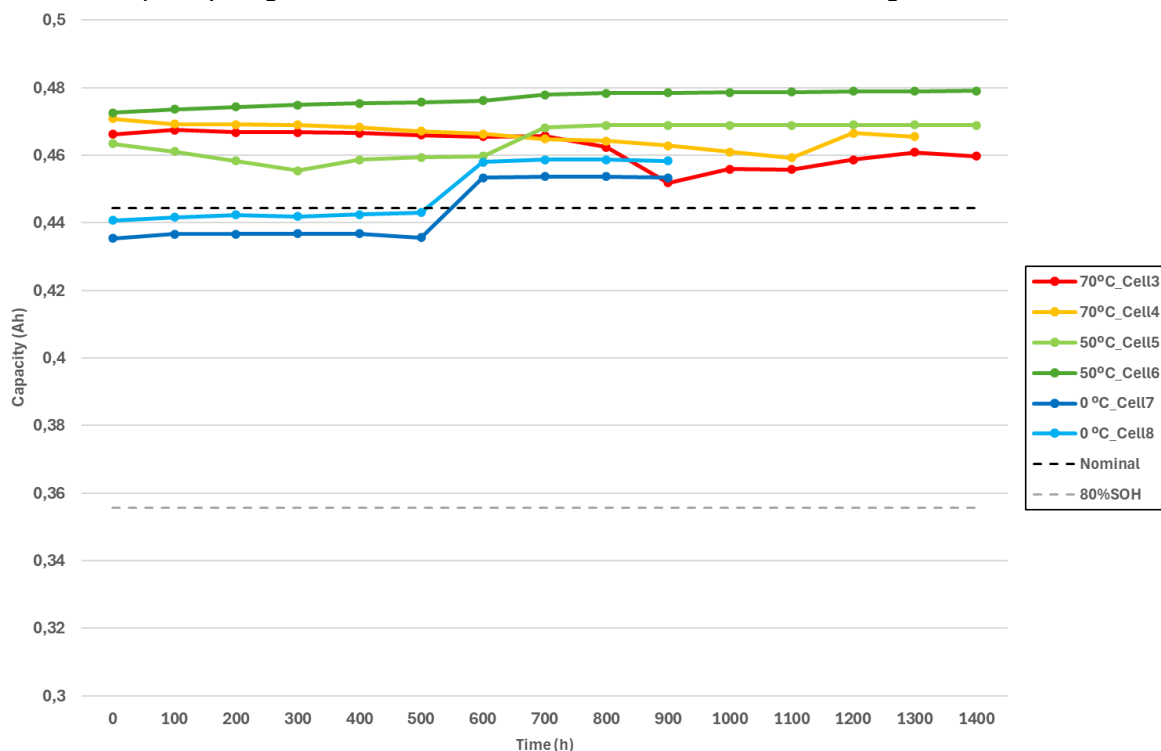
Figure 22. Capacity evolution at different floating temperatures vs. time

As it can be seen, when operating at temperatures of 50 ºC and 70 ºC, during the tests, cell capacity is higher than the nominal capacity of the cells. This reflects that the cells do operate better when subjected to high temperatures. In addition, during the 1400 h of the tests, in general, cells do not suffer from capacity decay. In the case of tests carried out at 70 ºC, after approximately 700-800 h, cells suffer a capacity decay, but it is later maintained quite constant at capacities around 0.46 Ah. This small capacity decay can be attributed to the test stop due to the maintenance period.

On the other hand, when analysing the results obtained for the tests carried out at 0 ºC, first, it can be seen that the capacities obtained are below the nominal capacity of the cells, which is in agreement with the results obtained in the electrochemical characterization in Figure 4. Furthermore, the capacity increase detected after 600 h of testing is attributed to the climatic chamber temperature change to 25 ºC due to internal problems.

In general, it can be checked that in any of the tests 80% of the nominal capacity has been obtained. Thus, no cell degradation has been achieved.

The internal resistance can also be another parameter associated to cell degradation. Thus, in the same way, after testing the cells at three different temperatures, the comparison of the obtained internal resistance within time can be checked in the following Figure 23:

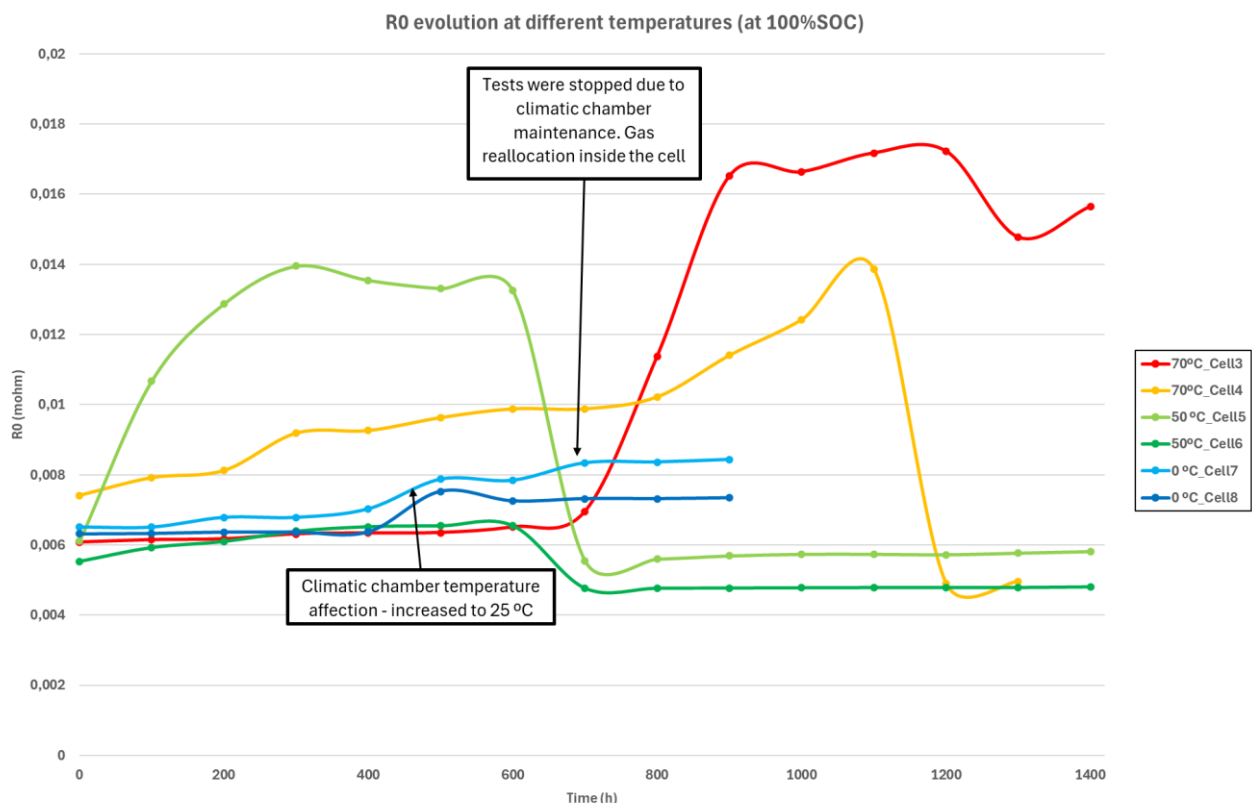Figure 23. Internal resistance evolution at different floating temperatures vs. time

As it can be seen, in general, when working at high temperatures (50 ºC and 70 ºC) cells internal resistance varies significantly among the two cells tested at the same conditions. Moreover, there is also a significant variation in the values over time. However, there is not a clear trend, thus, resistance variation can be multifactorial. One of the main reasons can be that cells are connected by crocodile connections (weak connection) and cell connection variability is reflected in an internal resistance change.

However, it should be noted that this internal resistance change is not related to cell degradation, since, as it can be checked in the Figure 22, no capacity degradation has been observed during the floating tests at any of the tested temperatures.

Thus, after keeping the cells under floating conditions for approximately 1400 h at three different temperatures, it can be concluded that no degradation has been observed in any case.

Finally, and concerting the Battery Thermal Management System (BTMS), a key factor is the relationship between thermal conductivity and the available surface area for heat exchange between the cell and the BTMS. In this case, according to the results found in terms of thermal conductivity, despite having a smaller surface area, it seems appropriate to take advantage of the much higher in-plane thermal conductivity through a system that facilitates heat exchange from the bottom or top of the cell instead of from the cell sides. This BTMS would contribute to remove heat faster while maintaining an homogeneous heat distribution among layers of the cell.

4 Recommendation

After conducting an exhaustive characterization of LICs, testing them under various operating conditions and conducting floating tests at three different temperatures, no significant signs of degradation were observed in the evaluated cells. These results highlight the excellent stability and robustness of LICs, even in scenarios simulating aggressive operating temperatures.

The absence of degradation is a promising indicator that supports the ability of these cells to maintain consistent performance over time, positioning them as a reliable technology for energy storage modules. However, the lack of degradation data poses a significant challenge in the development of advanced estimation algorithms that will be implemented in the i-SMS, particularly for SOH estimation. The accuracy of these algorithms heavily relies on models informed by degradation patterns, and the observed stability necessitates exploring alternative approaches to ensure effective long-term estimations.

Thus, to address this, available databases and public information on similar technologies will be analyzed as alternative sources of insights, which could help to develop the corresponding SOX algorithms. These algorithms will be implemented in the i-SMS, together with the balancing circuits and protections for the planned 12 V prototype module.

5 Risk register

Risk No.	What is the risk	Probability of risk occurrence[1]	Effect of risk[2]	Solutions to overcome the risk
WP7.1.1	Inability of degrading cells to develop algorithms for SOH estimation	High	Medium	Search for degradation data of non-commercial LICs in order develop the algorithms.

Table 6: Risk Register

---

[1] Probability risk will occur: 1 = high, 2 = medium, 3 = low

[2] Effect when risk occurs: 1 = high, 2 = medium, 3 = low

6 References

(1) Gustafsson, S. E. Transient Plane Source Techniques for Thermal Conductivity and Thermal Diffusivity Measurements of Solid Materials. *Review of Scientific Instruments* **1991**, *62* (3), 797–804. https://doi.org/10.1063/1.1142087.

(2) ISO-22007-2-2015.Pdf.

(3) Elkholy, A.; Sadek, H.; Kempers, R. An Improved Transient Plane Source Technique and Methodology for Measuring the Thermal Properties of Anisotropic Materials. *International Journal of Thermal Sciences* **2019**, *135*, 362–374. https://doi.org/10.1016/j.ijthermalsci.2018.09.021.

(4) Trofimov, A. A.; Atchley, J.; Shrestha, S. S.; Desjarlais, A. O.; Wang, H. Evaluation of Measuring Thermal Conductivity of Isotropic and Anisotropic Thermally Insulating Materials by Transient Plane Source (Hot Disk) Technique. *J Porous Mater* **2020**, *27* (6), 1791–1800. https://doi.org/10.1007/s10934-020-00956-3.

(5) Jannot, Y.; Acem, Z. A Quadrupolar Complete Model of the Hot Disc. *Meas. Sci. Technol.* **2007**, *18* (5), 1229–1234. https://doi.org/10.1088/0957-0233/18/5/009.

(6) Bryden, T. S.; Dimitrov, B.; Hilton, G.; Ponce De León, C.; Bugryniec, P.; Brown, S.; Cumming, D.; Cruden, A. Methodology to Determine the Heat Capacity of Lithium-Ion Cells. *Journal of Power Sources* **2018**, *395*, 369–378. https://doi.org/10.1016/j.jpowsour.2018.05.084.

(7) *What is Libuddy | Lithium-ion capacitor | JTEKT CORPORATION*. JTEKT CORPORATION. https://www.jtekt.co.jp/e/products/capacitor/capacitor_jtekt.html (accessed 2024-12-12).

7 Acknowledgement

Project partners

#	PARTICIPANT SHORT NAME	PARTNER ORGANISATION NAME	COUNTRY
1	CICE	CENTRO DE INVESTIGACION COOPERATIVA DE ENERGIAS ALTERNATIVAS FUNDACION, CIC ENERGIGUNE FUNDAZIOA	Spain
2	EUR	CLANCY HAUSSLER RITA	Austria
3	KIT	KARLSRUHER INSTITUT FUER TECHNOLOGIE	Germany
4	CNRS	CENTRE NATIONAL DE LA RECHERCHE SCIENTIFIQUE CNRS	France
4.1	IMN	NANTES UNIVERSITE (Affiliated)	France
5	UPS	UNIVERSITE PAUL SABATIER TOULOUSE III	France
6	FSU	FRIEDRICH-SCHILLER-UNIVERSITAT JENA	Germany
7	IRT-JV	INSTITUT DE RECHERCHE TECHNOLOGIQUE JULES VERNE	France
8	ELY	E-LYTE INNOVATIONS GMBH	Germany
9	BYD	BEYONDER AS	Norway
10	BCARE	BATTERYCARE S. L.	Spain
12	TALGO	PATENTES TALGO SL	Spain
13	UPC	UP CATALYST	Estonia

Table 7: Project Partners

8 Appendix A – Quality Assurance

The following questions should be answered by all reviewers (WP Leader, peer reviewer 1, peer reviewer 2 and the technical coordinator) as part of the Quality Assurance Procedure. Questions answered with NO should be motivated. The author will then make an updated version of the Deliverable. When all reviewers have answered all questions with YES, only then the Deliverable can be submitted to the EC.
NOTE: For public documents this Quality Assurance part will be removed before publication.

Question	WP Leader	Peer reviewer 1	Peer reviewer 2	Technical Coordinator
	Amaia Saenz de Buruaga	Jon Ajuria	María Arnaiz	Jon Ajuria
1. Do you accept this deliverable as it is?	Yes	Yes	Yes	Yes
2. Is the deliverable completely ready (or are any changes required)?	Yes	Yes	Yes	Yes
3. Does this deliverable correspond to the DoW?	Yes	Yes	Yes	Yes
4. Is the Deliverable in line with the MUSIC objectives?	Yes	Yes	Yes	Yes
a. WP Objectives?	Yes	Yes	Yes	Yes
b. Task Objectives?	No. It has been impossible to degrade commercial cells	No. It has been impossible to degrade commercial cells	No. It has been impossible to degrade commercial cells	No. It has been impossible to degrade commercial cells
5. Is the technical quality sufficient?	Yes	Yes	Yes	Yes